CLEO CONF 97-26
EPS97 337

Exclusive Reconstruction of $\bar{B} \to D^{(*)}\bar{D}^{(*)}K^-$

CLEO Collaboration

(August 1, 1997)

Abstract

We describe the first observation of decays of the form $\bar{B} \to D^{(*)}\bar{D}^{(*)}K^-$. We concentrate in particular on final states of the form $(D^0\bar{D}^0X)K^-$, where X denotes 0, 1, or 2 slow pions (charged or neutral). Signals are observed in several modes, and we are able to set interesting limits in others. This represents the first exclusive reconstruction of non-strange upper-vertex charm arising from the underlying $b \to c\bar{c}s$ process.

I. INTRODUCTION

The dominant process for hadronic $\bar{B}$ decay is the $b \to c\bar{u}d$ process, which yields a single D meson and light mesons from the $\bar{u}d$ hadronization (the 'upper vertex'). The $b \to c\bar{c}s$ process is phase-space suppressed, with a rate expected to be 20-30% of the $b \to c\bar{u}d$ rate [1]. A $b \to c\bar{c}s$ decay often results in upper-vertex production of a $D_s^{(*)-}$. The D_s^- and D_s^{*-} are both below threshold for $\bar{D}\bar{K}$ decay, but if a light-quark pair is popped between the $\bar{c}$ and the s, we may then produce a $\bar{D}\bar{K}$ pair. These $\bar{D}$ mesons will be characterized by their wrong charm flavor relative to the $\bar{B}$, and their softer momentum spectrum. In this analysis, we will attempt to perform exclusive reconstruction of such decays. The simplest final states are the three-body decays of the form $D^{(*)}\bar{D}^{(*)}\bar{K}^{(*)}$.

The motivation for this analysis is the 'charm-counting' problem in B-decays [1]. Briefly, the data on the inclusive charm yield from B decay and the inclusive semi-leptonic rate are somewhat inconsistent. A substantial amount of charm in B decays is due to $b \to c\bar{c}s$ and the inclusive measurements of charm yields should correctly include this. It is also worthwhile to investigate the amount of $b \to c\bar{c}s$ directly. We are interested in measuring the fraction of upper-vertex decays that can be accounted for as $D^{(*)}\bar{D}^{(*)}\bar{K}^{(*)}$ decays. Other goals include studying the $\bar{D}^{(*)}\bar{K}^{(*)}$ mass spectrum, the ratio of D and D^* at the lower vertex, and the ratio of K and K^* in these channels.

We caution the reader that the particle/anti-particle distinctions are important in this work. We use D ($\bar{D}$) as a generic term for D^0 and D^+ ($\bar{D}^0$ and D^-) only; we will always say D_s explicitly where needed. Charge-conjugate modes are always implied, but we are careful to maintain the proper B and D flavor correlations. In our terminology, a 'mode' is a specification of the exact $D^{(*)}$, $\bar{D}^{(*)}$, and $\bar{K}^{(*)}$ species in the final state. A 'sub-mode' refers to a particular way in which these three primary particles decay.

II. EXPECTATIONS FOR $\bar{B} \to D^{(*)}\bar{D}^{(*)}\bar{K}^{(*)}$

CLEO has presented an inclusive measurement of upper-vertex charm, using D-lepton correlations, which yields [3]:

$$B(\bar{B} \to \bar{D}X) = (7.9 \pm 2.2)\%. \tag{1}$$

LEP experiments have also provided data on inclusive rates. DELPHI has measured [4]:

$$B(\bar{B} \to D^{*+}D^{*-}X) = (1.0 \pm 0.2 \pm 0.3)\% \tag{2}$$

and ALEPH has measured [5]

$$B(\bar{B} \to D^0\bar{D}^0X, D^+\bar{D}^0X, D^0D^-X) = (12.8 \pm 2.7 \pm 2.6^{+0}_{-1.0})\%, \tag{3}$$

where the 3rd error is from a B_s contribution. Much of the observed rate is likely to appear in $D^{(*)}\bar{D}^{(*)}\bar{K}^{(*)}$ final states.

There are 6 possible 'base modes' of $\bar{B} \to D^{(*)}\bar{D}^{(*)}\bar{K}^{(*)}$ decay, for which we specify only the quark content of the mesons. The modes are summarized in Table I. In practice, we will restrict ourselves to pseudo-scalar and vector states, giving 8 varieties of each base mode.

TABLE I. The $D^{(*)}\bar{D}^{(*)}\bar{K}^{(*)}$ base modes. We use T (C) to denote color-allowed(-suppressed) amplitudes. Each D (K) may also be a D^* (K^*). For the color-allowed processes, we enclose the upper-vertex portion of the decay in ().

Mode	Mode	Amplitudes
$B^- \to D^0(\bar{D}^0 K^-)$	$\bar{B}^0 \to D^+(D^- \bar{K}^0)$	T,C
$B^- \to D^0(D^- \bar{K}^0)$	$\bar{B}^0 \to D^+(\bar{D}^0 K^-)$	T
$B^- \to D^+ D^- K^-$	$\bar{B}^0 \to D^0 \bar{D}^0 \bar{K}^0$	C

If we ignore color-suppressed processes, there are useful isospin relations. The spectator quark is irrelevant, so each B^- decay is equal in width to a corresponding $\bar{B}^0$ decay. The flavor of the quark popped at the upper vertex is also irrelevant, so that the two color-allowed modes for each charge of B have equal width. (See Ref. [2] for a more formal discussion.) Thus, the four color-allowed base-modes all have equal amplitudes, leaving eight independent amplitudes that correspond to the eight arrangements of pseudo-scalar and vector states.

Experimentally, the modes most accessible are those containing a K^- or K^{*0}. The isospin relations will allow us to use the rate determined in these modes to estimate the total rate into $D^{(*)}\bar{D}^{(*)}\bar{K}^{(*)}$. We concentrate here on the $D^{(*)}\bar{D}^{(*)}K^-$ modes, since these have the highest efficiency.

III. BASIC ANALYSIS AND COMMON CUTS

The important components of the CLEOII detector [6] for this analysis include three concentric drift chambers in a 1.5 T field for charged particle tracking, and a CsI calorimeter to measure electromagnetic showers. Particle identification is accomplished via specific ionization (dE/dx) in one of the wire chambers and time-of-flight (TOF) scintillators. The data sample used corresponds to $3.3 \times 10^6 B\bar{B}$ pairs.

Hadronic events are selected with loose criteria on track multiplicity and energy deposit. We further require $R2 < 0.4$, where $R2$ is the ratio of the 2^{nd} to 0^{th} Fox-Wolfram moments [7]. This event-shape cut is effective for reducing continuum background. $\bar{B} \to D^{(*)}\bar{D}^{(*)}\bar{K}^{(*)}$ decays are soft and result in a lower $B\bar{B}$ $R2$ (i.e., are more symmetric) than average $B\bar{B}$ events, hence the cut is very efficient for signal.

The sphericity angle, θ_{sph}, is the angle between the sphericity axis of the candidate and the remainder of the event [8]. Signal is flat in $cos(\theta_{sph})$, while background, especially continuum, is peaked near $cos(\theta_{sph}) = \pm 1$. This variable is useful if the continuum background is large; we require $|cos(\theta_{sph})| < 0.8$ only for the $D^0\bar{D}^0K^-$ mode.

We require that tracks are consistent with originating from the beam spot. Good dE/dx information is *required* and TOF information is used *if available*. We cut on consistency with the desired hypothesis (π or K) at 2.0, 2.5, or 3.0 standard deviations (σ), depending on the $D^{(*)}\bar{D}^{(*)}\bar{K}^{(*)}$ mode. For charged slow pions from D^* decay, we relax the beam-spot consistency cuts and do not use dE/dx or TOF information.

Showers not matched to tracks are used as photon candidates. The calorimeter is divided and used as follows:

- Good Barrel: $|cos(\theta)| < 0.71$; $E_\gamma > 30$ MeV

• Bad Barrel: $0.71 < |cos(\theta)| < 0.81$; $E_\gamma > 50$ MeV; at most one per π^0.
• Endcap: $|cos(\theta)| > 0.81$; not used
In addition, all photons must satisfy requirements on energy distribution and isolation; we remove showers consistent with being hadronic fragments or π^0's with merged photons.

Selected photons are paired to form π^0 candidates; those with an invariant mass within 2.5σ of nominal are kinematically fit constraining the mass to M_{π^0}. We require a successful fit in order to keep the candidate, and use the fit 4-vector in further analysis.

We form D^0 candidates from three standard modes:

$$K^-\pi^+, \quad K^-\pi^+\pi^0, \quad K^-\pi^-\pi^+\pi^+ \tag{4}$$

We look for D^{*+} (D^{*0}) in the $D^0\pi^+$ ($D^0\pi^0$) channel. All three D^0 sub-modes are employed. For D^0 (D^*), we cut on the deviation of the D mass ($D^* - D$ mass difference) from the nominal value; the expected resolution is calculated event-by-event from the track and shower error matrices. We cut at 2.0, 2.5, or 3.0σ, depending on the $D^{(*)}\bar{D}^{(*)}\bar{K}^{(*)}$ mode.

For the $D^0 \to K^-\pi^+\pi^0$ decay, we retain events only in high-amplitude regions of the Dalitz plot to reduce combinatorial background. Our requirement retains more than 75% of real decays in just 30% of the allowed phase space.

We exploit energy conservation by constructing

$$\Delta E = \sum E_i - E_{beam} = E_{measured} - E_{beam} \tag{5}$$

and perform a kinematic fit to ΔE with the D and D^* masses constrained. Typically, the resolution improves from about 15 MeV to 8 MeV. We employ cut of $|\Delta E| < 20$ MeV.

We use a beam-constrained mass technique to calculate M_B, which expresses momentum conservation:

$$M_B \equiv \sqrt{E_{beam}^2 - \left|\sum \vec{P}_i\right|^2}. \tag{6}$$

For purposes of identifying samples rich in signal events, studying other quantities such as $M_{\bar{D}\bar{K}}$, etc., we use a 2σ cut of ± 5 MeV/c^2 around the nominal B mass. The actual yields and significance are obtained from a fit, however, as described below.

We allow only one entry per sub-mode per event; the best entry is selected with a global event probability of χ^2 which is a sum of:
• The particle ID σ^2 for all (non-slow π) charged tracks, both dE/dx and TOF (when used).
• The σ^2 of the mass for each π^0, D^0, and $\bar{D}^0$ used.
• The σ^2 of the mass difference $\delta m \equiv M_{\pi K\pi(\pi^0)} - M_{K\pi(\pi^0)}$ for any D^* or $\bar{D}^*$.
We have intentionally avoided using ΔE in the selection, to prevent clustering of background near $\Delta E = 0$; we prefer to leave the ΔE vs. M_B plane undistorted.

The probability of χ^2 variable is also very powerful in separating signal and background. We use a modified χ^2 to calculate the probability: all of the pion particle ID quantities are removed. The tracks are usually true pions, and only dilute the separation. We require a probability greater than 5% for all candidates.

Of the 12 possible $D^{(*)}\bar{D}^{(*)}K^-$ modes, we study those with no $D^\pm$ in the final state. This leaves 7 modes of the form $(D^0\bar{D}^0X)K^-$, where X denotes possible slow pions from D^* decays. The only case in which we use multiple sub-modes in this analysis is for the $D^0/\bar{D}^0$, leading to 9 sub-modes possible for every mode.

IV. FINAL CUTS AND YIELD EXTRACTION

Final cuts adjustments for each mode are done primarily on the particle ID and mass requirements. The $K^{\pm}$ particle ID quantities are useful, since many $K^{\pm}$ are soft enough to allow good K/π discrimination, and since there are three per event. Because most of the D and D^* candidates are combinatoric fakes, tightening requirements on the D mass and D^*-D mass-difference is also quite helpful.

To tune the requirements, we look at the number of background events expected according to Monte Carlo, compared to the number of signal events expected (with an assumed branching fraction of 0.5 to 1.0 %). We also monitor the distribution of background events across the sub-modes. If the background is too high, we begin to tighten cuts and throw out the noisiest sub-modes, aiming for ≤ 1 event background while maintaining high efficiency. Generally, there is a natural grouping into low- and high-background sub-modes. We avoid sub-mode dependent cuts. The $K^{\pm}$ particle ID, the D mass, and the $D^* - D$ mass difference are each set to either 2.0, 2.5, or 3.0σ as a result of these studies.

The yield in each mode is obtained from a joint likelihood fit to two M_B distributions. The first distribution has $|\Delta E| < 20$ MeV and contains the signal. The second satisfies $30 < |\Delta E| < 110$ MeV, and is used to constrain the background shape. The ΔE distribution is fairly flat, and we only use the sidebands for the background shape, not for normalization. Analysis cuts (except the sub-mode selection cut) are loosened for the sidebands to obtain larger statistics. The fit includes a common background shape for both M_B distributions and a single signal Gaussian for the M_B distribution in the ΔE signal region.

The mean of the Gaussian is fixed to 5.280 GeV/c^2, and the width is fixed to 2.5 MeV/c^2, which was determined from signal Monte Carlo. We use 0.5 MeV/c^2 bins to avoid binning effects, although we plot in wider bins for display purposes. In order to evaluate the significance, we re-fit with the signal Gaussian area set to 0 but other parameters still floating, and convert the change in the likelihood to a significance. In the one case of low statistics, we use standard Poisson methods to extract a limit.

V. EFFICIENCIES AND DATA YIELDS

The fits to the M_B distribution of each mode are shown in Figure 1. The resulting yields and significances are summarized in Table II. The net 'sensitivity' listed for each $D^{(*)}\bar{D}^{(*)}K^-$ mode in Table II is $10^4 \times \sum(\epsilon_i \times \prod BR_i)$, where the ϵ_i is the reconstruction efficiency, $\prod BR_i$ is the product of the relevant sub-mode branching fractions, and the index i runs over all sub-modes used. A fit to all seven modes yields $23.0^{+5.6}_{-4.9}$ events with a significance of 7.5σ.

In Figure 2, we display plots for the sum of all seven modes. The M_B and ΔE distributions show clear signal peaks. One also notes a satellite peak at $\Delta E \simeq -M_\pi$ due to events with a missing soft pion from a D^*. The $\bar{D}\bar{K}$ mass distribution shows no discernible features beyond the naively expected phase-space behavior. Similar plots are examined for other data samples. We see no peaking in the off-resonance data (taken below the $\Upsilon(4s)$ resonance), verifying that these are B decays. We also see no signal in our nominal $B\bar{B}$ Monte Carlo, which does not explicitly contain $D^{(*)}\bar{D}^{(*)}K^-$ decays.

TABLE II. For each mode, we list the sensitivity, total fit yield, and significance. 'Sensitivity' is defined in the text.

Mode	# sub-modes used	Sensitivity	Yield	Significance
$D^{*+}\bar{D}^0K^-$	5	3.4	5.08+2.85−2.16	3.5
$D^{*0}\bar{D}^0K^-$	5	2.2	4.29+2.59−1.93	3.1
$D^{*+}\bar{D}^{*0}K^-$	8	1.4	6.39+2.99−2.33	4.5
$D^{*0}\bar{D}^{*0}K^-$	6	1.0	4.84+2.58−1.92	4.4
$D^0\bar{D}^{*0}K^-$	5	2.2	1.99+2.02−1.33	1.8
$D^0\bar{D}^0K^-$	1	2.3	0.42+1.40−0.75	0.5
$D^{*+}D^{*-}K^-$	8	1.1	0	0

TABLE III. The sub-mode branching fractions used.

Mode	Branching Fraction (%)	Reference
$\mathcal{B}(D^{*0} \to D^0\pi^0)$	63.6 ± 4.0	[9]
$\mathcal{B}(D^{*+} \to D^0\pi^+)$	68.1 ± 1.6	[9]
$\mathcal{B}(D^0 \to K^-\pi^+)$	3.91 ± 0.11	[10]
$\mathcal{B}(D^0 \to K^-\pi^+\pi^0)/\mathcal{B}(D^0 \to K^-\pi^+)$	3.81 ± 0.19	[11]
$\mathcal{B}(D^0 \to K^-\pi^-\pi^+\pi^+)/\mathcal{B}(D^0 \to K^-\pi^+)$	1.97 ± 0.10	[12]

The branching fractions for the necessary sub-modes are taken from the most recent CLEO measurements with the exception of $\mathcal{B}(D^0 \to K^-\pi^-\pi^+\pi^+)/\mathcal{B}(D^0 \to K^-\pi^+)$, where we use the PDG average. The values are listed with references in Table III. For the values of $\mathcal{B}(D^0 \to K^-\pi^+)$ and $\mathcal{B}(D^0 \to K^-\pi^+\pi^0)/\mathcal{B}(D^0 \to K^-\pi^+)$, we list the total error used after removing some correlated errors (see below).

VI. FEED-ACROSS BETWEEN MODES

One source of feed-across between modes arises from a slow pion being replaced with a random particle of a different charge. If the accidental slow pion was the same charge as the correct one, this is counted as part of the efficiency. After cuts, this source peaks well in ΔE and M_B. This feed-across is evaluated with signal Monte-Carlo. Most feed-across occurs between modes with the same number of D^*'s.

The γ from the decay $D^{*0} \to D^0\gamma$ may also be replaced with a fake slow π to make a D^* of either charge. We have analyzed samples of signal Monte Carlo with $D^{*0} \to D^0\gamma$ decays; the distributions in M_B and ΔE clearly peak, but are about 2.5 times broader than the real signal. This feed-across rate is also evaluated with the Monte Carlo. Note that the processes $D^{*+} \to D^+\pi^0$ and $D^{*+} \to D^+\gamma$ are not problematic, since we do not use any D^+'s when reconstructing D^*'s.

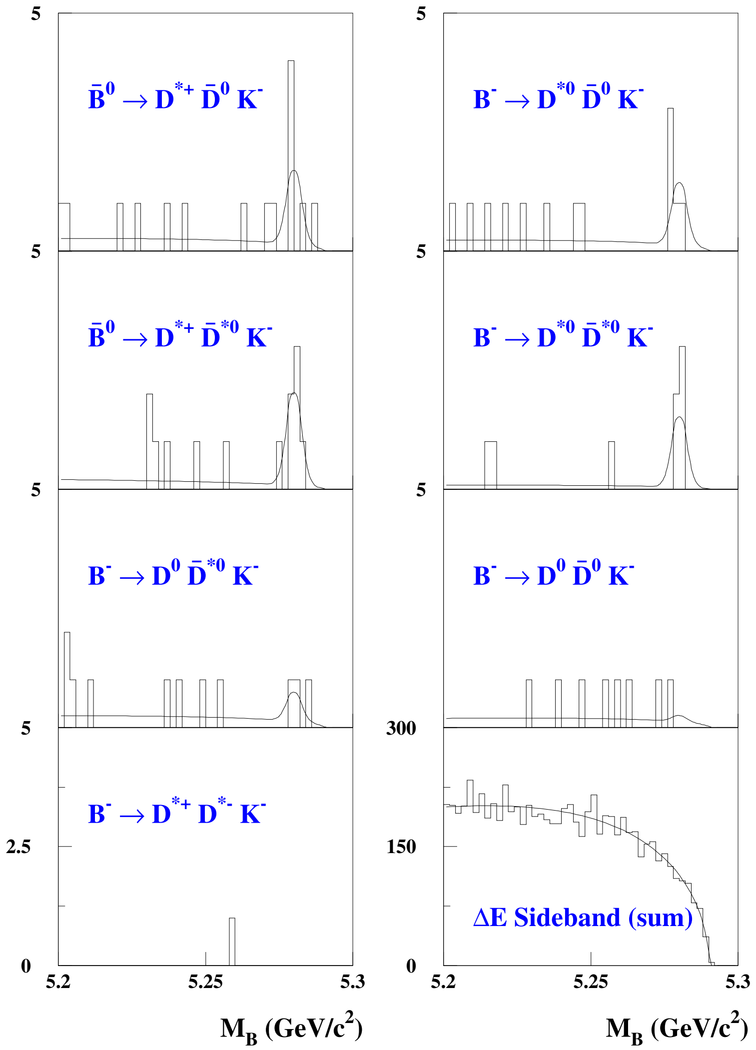

FIG. 1. The fits to the B mass distribution for the seven modes.

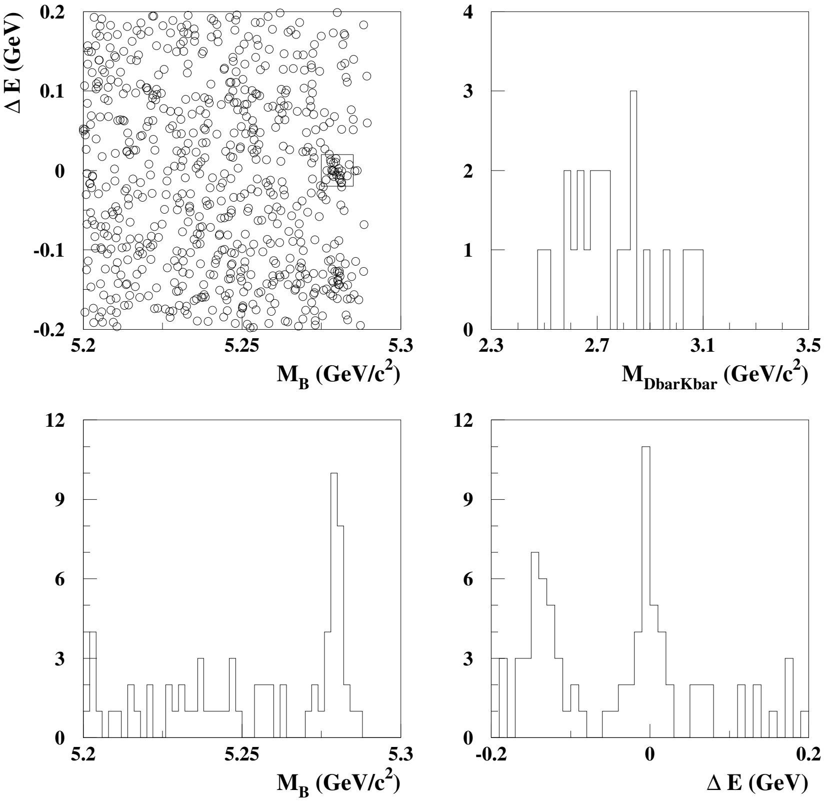

FIG. 2. Sum of all seven $(D^0\bar{D}^0X)K^-$ modes, in data. The box in the M_B vs. ΔE plot shows the signal region used for the $M_{\bar{D}\bar{K}}$ distribution.

Another potential concern is feed-across between different sub-modes within the same $D^{(*)}\bar{D}^{(*)}K^-$ mode. We check for this in our signal Monte Carlo and observe no effect.

We do not know of any other source of significant feed-across other than the scenarios described involving fake slow pions. $D^{(*)}\bar{D}^{(*)}\pi^-$ is Cabibbo-suppressed, and the ΔE resolution is sufficient to separate it from the signal (in the worst case the shift in ΔE is about 10σ). We know of no other mechanism to fake these $D^{(*)}\bar{D}^{(*)}K^-$ modes.

The size of the corrections is summarized below in our discussion of systematics.

VII. SYSTEMATIC ERRORS

The systematic errors considered are summarized in Table IV. We include an error from the Monte-Carlo statistics used to determine the efficiency, as indicated.

The sources of uncertainty in our reconstruction efficiency are summarized in Table V. All errors that are 'per track', etc., are taken as completely correlated within a given decay, as are the normal track and slow-π finding errors. The self-correlations for all errors are also maintained across all sub-modes.

TABLE IV. Systematic Errors. All errors are relative to the branching fraction.

Mode	MC Stats %	Efficiency %	Sub-Mode BR %	Feed-Across %	Total %
$D^{*+}\bar{D}^0K^-$	3.6	13.9	6.9	2.9	16.2
$D^{*0}\bar{D}^0K^-$	4.2	16.0	8.9	11.0	21.8
$D^{*+}\bar{D}^{*0}K^-$	4.9	16.1	9.7	7.0	20.6
$D^{*0}\bar{D}^{*0}K^-$	5.3	16.9	14.2	8.4	24.2
$D^0\bar{D}^0K^-$	7.6	12.1	5.4	–	15.3
$D^0\bar{D}^{*0}K^-$	4.2	16.0	8.9	–	18.8
$D^{*+}D^{*-}K^-$	6.7	17.6	8.4	–	20.7

TABLE V. Systematic Errors on Efficiency.

Item	error (%)	comment
Track-finding	1.0% per track	
Slow-$\pi^\pm$-finding	5.0% per track	
π^0-finding	5.5% per π^0	
$K^-\pi^+\pi^0$ Dalitz cut	5.0% per D^0	
dE/dx Particle ID	0.5/1.0/1.5% per track	shown for 3.0/2.5/2.0 σ cut
TOF Particle ID	1.0/1.5/2.0% per track	shown for 3.0/2.5/2.0 σ cut
D mass cut	1.0/2.0/4.0% per D	shown for 3.0/2.5/2.0 σ cut
$D^* - D$ mass diff. cut	1.0/2.0/4.0% per D^*	shown for 3.0/2.5/2.0 σ cut
Prob(χ^2) sort and cut	3.0%	
ΔE cut	3.0%	

We have worried about some of the correlated systematics arising from the sub-mode branching fractions, most of which are also taken from CLEO measurements. To first order, we may remove the track-finding and π^0-finding errors from the CLEO branching fractions for $D^0 \to K^-\pi^+$, $D^0 \to K^-\pi^+\pi^0$ and count them only in our current analysis. We have done this and assume that all other errors from the sub-mode branching fractions are uncorrelated.

The error on the feed-across is substantial, largely due to the statistical errors on the branching fractions and feed-across rates and systematic effects in determining how the events are counted in the yield fits. We assume a 100% error on the feed-across to cover these uncertainties. The results are summarized in Table IV. We have ignored the feed-across correction to the upper-limits, which results in conservative limits.

For modes with observed signals, we correct the branching fraction for feed-across, and add the feed-across error in quadrature with the other systematic errors. To obtain upper limits, we have integrated the likelihood function, after accounting for the systematic error from Monte Carlo statistics, efficiency systematics and sub-mode branching-fraction systematics.

Finally, we caution that all reconstruction efficiencies are determined with phase-space Monte-Carlo samples. The observed signal events seem to populate Dalitz plots uniformly, and the efficiency does not vary too greatly across the plots. However, we have not included any possible bias in the systematics for this preliminary result.

VIII. CONCLUSIONS

Combining all of the above pieces, we arrive at the following preliminary results, where we assume phase-space for determining efficiencies:

- $\mathcal{B}(\bar{B}^0 \to D^{*+}\bar{D}^0 K^-) = (0.45^{+0.25}_{-0.19} \pm 0.08)\%$
- $\mathcal{B}(B^- \to D^{*0}\bar{D}^0 K^-) = (0.54^{+0.33}_{-0.24} \pm 0.12)\%$
- $\mathcal{B}(\bar{B}^0 \to D^{*+}\bar{D}^{*0} K^-) = (1.30^{+0.61}_{-0.47} \pm 0.27)\%$
- $\mathcal{B}(B^- \to D^{*0}\bar{D}^{*0} K^-) = (1.45^{+0.78}_{-0.58} \pm 0.36)\%$
- $\mathcal{B}(B^- \to D^0\bar{D}^0 K^-) < (0.5)\% \quad (90\% CL)$
- $\mathcal{B}(B^- \to D^0\bar{D}^{*0} K^-) < (0.8)\% \quad (90\% CL)$
- $\mathcal{B}(B^- \to D^{*+}D^{*-} K^-) < (0.7)\% \quad (90\% CL)$

The first error is statistical; the second is systematic, including efficiency, branching fraction, and feed-across systematics.

We see a total $B \to D^*\bar{D}^{(*)0}K^-$ branching fraction of about 2% per B charge (B^- or $\bar{B}^0$). Applying upper-vertex isospin (i.e., equating $\bar{D}^{(*)}K^-$ with $D^{(*)-}\bar{K}^0$), this accounts for 4% per B charge. As yet unaccounted for are modes where the lower vertex is a D (not a D^*), for which we only have limits, and modes with a K^*, which we have not yet investigated.

Now that the existence of the modes has been established firmly, the goal for the future is to determine the total rate of $\bar{B} \to D^{(*)}\bar{D}^{(*)}\bar{K}^{(*)}$. All signals are currently of the form $D^*D^{(*)}K$. We need the ratio of lower-vertex D/D^* and the ratio of K^*/K in order to complete the picture. It is also important to search for the color-suppressed modes; only one such mode has been looked at thus far. Final state interactions may play a role in populating color-suppressed modes since the decay products are relatively soft.

In conclusion, we find that $D^{(*)}\bar{D}^{(*)}\bar{K}^{(*)}$ modes account for a significant fraction of the inclusive wrong-sign charm production in B decays. It is not yet clear how fully they saturate it.

ACKNOWLEDGMENTS

We gratefully acknowledge the effort of the CESR staff in providing us with excellent luminosity and running conditions. J.P.A., J.R.P., and I.P.J.S. thank the NYI program of the NSF, M.S. thanks the PFF program of the NSF, G.E. thanks the Heisenberg Foundation, K.K.G., M.S., H.N.N., T.S., and H.Y. thank the OJI program of DOE, J.R.P., K.H., M.S. and V.S. thank the A.P. Sloan Foundation, R.W. thanks the Alexander von Humboldt Stiftung, and M.S. thanks Research Corporation for support. This work was supported by the National Science Foundation, the U.S. Department of Energy, and the Natural Sciences and Engineering Research Council of Canada.

REFERENCES

[1] Gerhard Buchalla, Isard Dunietz and Hitoshi Yamamoto, Phys. Lett. **B364**, 188 (1995).
[2] Isard Dunietz, FERMILAB-PUB-96/104-T (hep-ph/9606247).
[3] CLEO Collaboration, CLEO CONF 97-27.
[4] DELPHI Collaboration, XXVIII ICHEP (Warsaw), 1996, contributed paper PA01-108.
[5] ALEPH Collaboration, XXVIII ICHEP (Warsaw), 1996, contributed paper PA05-060.
[6] Y. Kubota, *et al.*, Nucl. Instrum. Methods A **320**, 66 (1992).
[7] G. Fox and S. Wolfram, Phys. Rev. Lett. **41**, 1581 (1978).
[8] G. Hanson, *et al.*, Phys. Rev. Lett. **35**, 1609 (1978); S.L. Wu and G. Zobernig, Z. Phys. C **2**, 107 (1979).
[9] CLEO Collaboration, F. Butler, *et al.*, Phys. Rev. Lett. **69**, 2041 (1992).
[10] CLEO Collaboration, D. Akerib, *et al.*, Phys. Rev. Lett. **71**, 3070 (1993).
[11] CLEO Collaboration, B. Barish, *et al.*, Phys. Lett. **B373**, 334 (1996).
[12] 1996 Review of Particle Physics, R.M Barnett, *et al.*, Phys. Rev. D **51**, 1 (1996).